

Evaluation of mechanical and thermal properties of thermoplastic polymer composites

3

Pragya Sharma¹, V.K. Singh¹, Sakshi Chauhan¹ and Naman Jain²

¹Department of Mechanical Engineering, College of Technology, Govind Ballabh Pant University of Agriculture and Technology, Pantnagar, Uttarakhand, India, ²Department of Mechanical Engineering, ABES Engineering College, Ghaziabad, Uttar Pradesh, India

3.1 Introduction

A composite material is created by combining several substances to create a substance that has properties that are superior to those of the constituent substances (Dagdag et al., 2019; Hsissou, About et al., 2021; Khalil et al., 2013). Reinforcement arrangements, which are composite materials embedded in a matrix, is now a frequently used term (Dagdag et al., 2020; Hsissou et al., 2020). The cohesion and orientation of the load are guaranteed by the matrix. Furthermore, it is possible to transmit the load with the stresses that its composite is experiencing. The resultant materials are frequently anisotropic and very heterogeneous (Amrollahi et al., 2019; Hsissou et al., 2019; Le Guen et al., 2016; Rod et al., 2019). The parameters that can affect the qualities of the composite include the kind of matrix and charge, charge form and proportion, interface quality, and production method (Asim et al., 2018; Khalil et al., 2011; Venkateshwaran & Elayaperumal, 2010). The matrix and reinforcement can be composed of metals, ceramic, or plastic, which opens up a wide range of possible combinations (Chen & Gao, 2019; Cheng et al., 2020; Devnani & Sinha, 2019; Li et al., 2018). The composite material typically consists of a continuous phase as well as one or more discontinuous phases. The composite is considered as a hybrid when it has many discontinuous stages of various types (Ahmadijokani et al., 2020; Arabpour et al., 2020; Dong et al., 2019; Li et al., 2018). The continuous phase is referred to as the matrix, and the discontinuous phase is known as the reinforcement or reinforcing material. Components with comparable mechanical and physical properties are combined to create composite materials (Baek et al., 2020; De et al., 2020). The mechanical and thermal properties can be enhanced by adding reinforcements with significant modularity and excellent tensile strength to a polymer matrix (Das & Tiwari, 2019; Datsyuk et al., 2020; El Gouri et al., 2009; Hsissou & El Harfi, 2018; Hsissou, Bekhta et al., 2017; Hsissou, Benassaoui et al., 2017; Hsissou, El Bouchti et al., 2017; Hsissou, Bekhta, & El Harfi, 2018; Hsissou, Bekhta & Elharfi, Benzidia, et al., 2018). The benefit of composites with a polymer matrix overmetals is the method of

manufacture, which facilitates the fabrication of parts with complicated geometries and lower densities, reducing fuel consumption (for aeroplanes and vehicles), increasing speeds in competitive sport, or extending the range and payload of missiles (in transport) (Tarhini & Tehrani-Bagha, 2019; Vaggar & Kamate, 2019; Wu & Drzal, 2016; Zhang et al., 2019). These composite materials have an impact on a variety of application fields, including packaging, automotive, gentle structures, structural engineering, aviation, sports, biomedical, thermal-mechanical components, and aerospace.

The matrix might be made of an elastomer, thermoplastic, or thermosetting material. The matrix links the reinforcing fibers, disperses the constraints, provides chemical resistance for the structure, and gives the finished product the desired shape (Arabpour et al., 2020; Zheng et al., 2019). The function that the composite material is intended to serve determines the matrix that is employed. The thermoplastic matrices' linear chains are malleable while they are still in the melting process. In the majority of industrial processes, thermoplastic matrices are heated, after which the finished product is molded utilizing injection, extrusion, or thermoforming processes and is then cooled to maintain its shape. This procedure is reversible. The processing of these materials should be easier and quicker because thermoplastics completely respond to high-molecular-weight resins that do not conduct chemical reactions during curing. Thermoplastics can be thermoformed and consolidated in a matter of minutes (or even seconds), whereas thermosets need lengthy cures (hours) to allow for the chemical reactions that create molecular weight and crosslinking. Due to the thermoplastics' complete reaction, they do not contain any tack, making the prepreg stiff and board-like. Thermoplastics are available in a wide range of forms today, each with a distinctive set of fascinating characteristics. They can be manufactured as transparent as glass, as stiff as metal and concrete, or as flexible as rubber to be used in a range of goods. They produce excellent thermal and electrical insulators, have good corrosion resistance, and do not rust. Fig. 3.1 shows formulation of composite materials on the basis of reinforcements, additives, and matrices (Hsissou, Seghiri et al., 2021). The following subcategories of thermoplastic polymers are also possible: (1) commodity or all-purpose plastics such acrylonitrile butadiene styrene resin, polystyrene, polypropylene (PP), and polyethylene. Polyamide, polyethylene terephthalate, polycarbonate, polyetheretherketone (PEEK), polyetherimide, polyethersulfone (PES), and polyphenylene sulfide are examples of high performance or engineering plastics (Park & Heo, 2014; Rajak et al., 2019; Yao et al., 2018). Thermoplastics are an excellent material for many applications due to their light weight, great mechanical strength, and resilience to environmental factors.

3.2 Physical properties

Physical characteristics are significant; one must understand the necessary length, width, and weight for a specified part or product. For instance, it must be light enough to manage accurately when utilized by a surgeon because lighter materials make material implementation considerably simpler and less dangerous (McKeen,

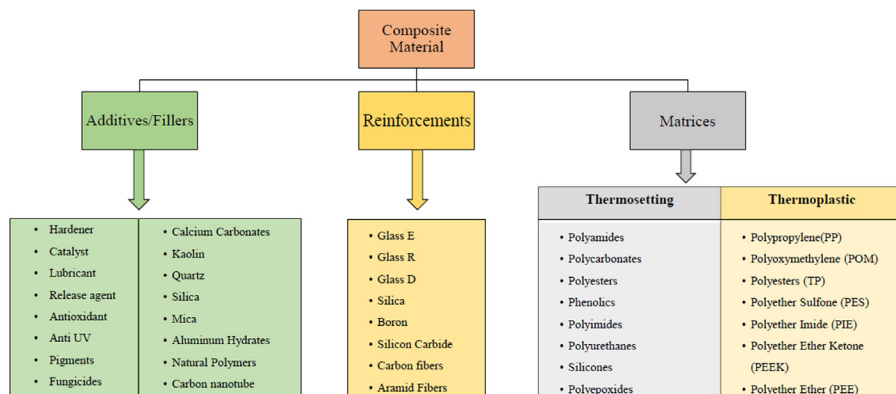


Figure 3.1 Formulation of composite materials on the basis of reinforcements, additives, and matrices.

Table 3.1 24 hours water absorption and thickness swelling of LCNF/Pebax nanocomposites (Farsi et al., 2018).

Lignocellulose nanofibers (%)	Water absorption (24 h) (%)	Thickness swelling (24 h) (%)
0	1.75	2.94
1	1.63	3.01
3	0.88	2.63
5	0.95	2.22

2014). Due to the high transportation costs associated with high-density values, density can also be a very crucial design component. By multiplying mechanical qualities by the appropriate density, density is frequently used to calculate “particular attributes”. Furthermore, these precise characteristics help one understand the inherent strength of the building they intend to design (Van de Velde & Kiekens, 2002).

Mohammad Farsi et al. studied the properties of biodegradable composites using Pebax thermoplastic elastomer and lignocellulose nanofibers (LCNFs). For this, LCNFs at various levels of 0%, 1%, 3%, and 5% were taken into consideration. Benzyl alcohol was used to prepare the LCNFs before they were combined with Pebax. The findings of the physical characteristics test showed that adding additional LCNF reduced the thickness swelling and water absorption. Table 3.1 displays the polyether-b amide composites reinforced with LCNF after a 24-hour soaking in water in terms of water absorption and swelling in thickness. The pure polymers without LCNF was tested, and this resulted in maximum water absorption. The water absorption reduced when the LCNF was increased to 3%, but it slightly increased when the LCNF loading was raised from 3% to 5%. The polymer

specimens 1% of LCNF had the largest thickness swelling (3.01%), and as LCNF loading increased, the thickness swelling decreased until it reached its lowest value (2.22%) at 5% of LCNF (Farsi et al., 2018).

Helen et al. analyzed the usage of polyvinyl alcohol (PVA) for direct methanol fuel cells, which involved creating a membrane out of PVA, zirconium phosphate, and the cesium salt of heteropoly acid. 10 wt.% of zirconium phosphate and 30 wt.% of orthophosphoric acid were mixed in a 10 wt.% PVA solution with water, and then the mixture was stirred at 343K for 8 hours to make the film. The PVA-based membrane was subjected to a water absorption test by being submerged in deionized water for 2 hours; the results showed that the PVA-ZrP-Cs1-SWA hybrid membrane absorbed roughly 240% more water than the PVA-ZrP-Cs2-SWA hybrid membrane. Studying the impact of crosslinking on the swelling degree revealed that the swelling degree ranged between 68% and 76%, and films containing a greater content of PVA indicate a greater swelling degree. Crosslinking was accomplished by soaking the membrane in 0.5 weight by volume% TMC/hexane. Studying the impact of glyoxal crosslinking upon composite swelling power revealed that swelling power decreased with crosslinking from plain PVA to crosslinked PVA from 105.6% to 78.3%, and that the swelling degree of crosslinked MFC-PVA was found to be 75.1% (Helen et al., 2006). According to research by Abdulkhani et al. on water absorption qualities, cellulose/PVA film has a greater water absorption rate than cellulosic film, ranging from 73% to 78% compared to 33% to 42% for cellulosic film. This difference is likely caused by the presence of -OH (Abdulkhani et al., 2013). Tian et al. investigated how starch affected the amount of water that a PVA blended with starch film absorbed. The extent of crystallinity of the PVA component reduced with an increase in starch, as did the water intake at equilibrium. The water intake of the resultant blends at equilibrium increased with an increase in RH (Tian et al., 2017). Amorphous or semicrystalline polymers are both possible. Regular repeating units in semicrystalline polymers enable the chains to fold into crystallites, which are dense areas. In comparison to an amorphous counterpart, they serve as crosslinks to provide the polymer better tensile strengths and greater modulus. Semicrystalline polymers nevertheless contain amorphous regions since no polymer can fully organize into a totally crystalline substance (Middleton & Tipton, 2000). Depending on the stereochemistry and thermal properties, PLA can either be amorphous or semicrystalline in the solid state. The T_g establishes the highest use temperature for amorphous PLAs in the majority of industrial applications. The T_g (58°C) and T_m (130°C–230°C, based on structure) of semicrystalline PLAs are crucial for defining the use of temperatures for various applications. The overall optical composition, fundamental structure, thermal properties, and Mw have a significant impact on these two transitions, T_g and T_m . Amorphous PLAs behave as a viscous fluid when heated above T_g , when they change from glassy to rubbery. When PLA is cooled to its transition temperature, which is around 45°C, it begins to behave like glass and creeps. PLA only exhibits brittle polymer behavior below this temperature (Henton et al., 2005). Siti Nikmatin et al. investigated the impact of a nanoparticle-sized rattan filler on the mechanical, thermal, and physical characteristics of the composite. Considerations were neat PP,

PP mixed with 5 wt.% rattan nanoparticle (PP/R5), and PP mixed with 5 wt.% glass fiber (PP/FG5). Particle size analysis, morphology, X-ray diffraction, thermal inspection, and mechanical testing were done to evaluate performance. In PP/R5, the highest level of crystallinity was found. Comparing PP and PP/FG5, it was found that PP/R5 displayed the highest level of crystallinity. The PP/surface R5 morphology was generally well distributed and therefore superior to the other materials taken into consideration. This is supported by the fact that PP/R5 had the greatest average Rockwell hardness (Nikmatin, 2017).

3.3 Thermal properties

Using Pebax thermoplastic elastomer and LCNFs, Mohammad Farsi and colleagues investigated the characteristics of biodegradable composites (LCNFs). LCNFs at varied levels of 0%, 1%, 3%, and 5% were considered for this. Before being mixed with Pebax, the LCNFs were prepared in benzyl alcohol. As the content of LCNF fluctuated, there was no discernible pattern in the variations in enthalpy. The temperature of crystallization increased as the LCNF content was raised to 5%. Glass transition temperature (T_g) dropped when LCNF content grew to 3%; however, T_g increased with the addition of more LCNFs. Peaks at 1740 cm^{-1} were visible in the infrared spectra produced by the Fourier transform, which indicated the presence of polyamide bonds (Farsi et al., 2018). R. Mahesh Kumar et al. had done thermal research on thermoplastic rubber (TPR) and its composites. TPR is a substance that exhibits a thermoplastic character above its melting point and has elastomeric conductivity within its specified temperature range without cross-linking during manufacture. Being the most effective filler particle in the composite, PTFE particles are used in high-temperature applications. Injection molding techniques were used to create samples of 100% TPR and 10%, 20%, and 100% mixed specimens of PTFE and TPR. Based on test results, it is clear that composites with a PTFE filler exhibit strong heat conductivities. The thermogravimetric analysis (TGA)-obtained thermal characteristics graphs show that PTFE particle-reinforced composites made of TPR polymers have considerably improved thermal properties (Thermal Properties of Thermoplastic Rubber TPR Reinforced with Polytetrafluoroethylene PTFE Particle Polymer Composite, 2019). Anjum Saleem et al. used thermoplastic polymers, such as PEEK and PES, which were melt-blended with carbon fibers (CFs) to create composites. The mechanical, thermal, and electrical characteristics of these composites were examined. Differential scanning calorimetry (DSC) and TGA measurements of thermal characteristics were made. These techniques aid in understanding how fiber composition and fiber-matrix adhesion in composites affect the final product. Because CFs make composites electrically and thermally conductive, these properties were also investigated in the composites. Because of the strong link between the matrix and the reinforcement, DSC thermograms revealed that the inclusion of fillers has reduced melting peaks. Exothermic peaks

for PEEK/CF indicate cold crystallization. The DSC curve steepens at a temperature around 213°C, signaling the impending glass transition temperature (Saleem et al., 2007). By using CNFs as a nanofiller and thermoplastic starch as a nanocomposite, Kaushik et al. created biodegradable nanocomposites with three distinct CNF loadings: 5, 10, and 15 wt.%. The CNFs mentioned in their paper were recovered from wheat straw using a mixture of mechanical, chemical (alkali and acid hydrolysis and bleaching), and steam explosion (homogenization). Researchers looked at the produced nanocomposites' morphological, structural, mechanical, thermal, and moisture retaining characteristics. Using the use of transmission electron microscopy (TEM), the nanoscale dimensions of CNFs were examined. The results showed that the fibers had an agglomeration propensity and a diameter between 10 and 60 nm. Once the loading reached 10 wt.%, the barrier property started to deteriorate and continued to do so as the CNF concentration rose. The nanocomposite's CNF fiber aggregation was blamed for this. TGA and DSC were used to examine the thermal characteristics of nanocomposites. The connection between glycerol and CNF is revealed by the thermal property investigation. The TGA data revealed that the initial degradation temperature remained constant till the concentration of CNF-10 weight% was achieved, after which the temperature decreased in comparison to pure starch. They offered two potential explanations for this decline: (1) the decreased flexibility of branching amylopectin caused by nanocrystalline cellulose and (2) the buildup of the plasticizer (glycerol) on the CNF surface (Kaushik et al., 2010). It is well investigated how adding nanofillers like clay or nanocellulose might improve the performance of biocompatible polymers like polycaprolactone (PCL). Unaltered cellulose nanowhiskers (CNWr) and poly-ester bonded CNWr (CNWr-g-PCL) were used to create PCL-based nanocomposites at three different concentrations in the PCL matrix: 2, 4, and 8 wt.% each. Ramie fibers were hydrolyzed in alkaline and acid to produce CNWr. Lastly, the nanocomposites were created by melt mixing PCL and the nanofillers at 120°C. The melting and crystallization properties of the nanocomposites using CNWr as nanofiller did not vary significantly. The concentration of CNWr-g-PCL rose along with a small rise in crystallization temperature. The produced nanocomposite's thermomechanical characteristics were significantly enhanced by the grafted nanofiller (Goffin, 2011). Clay-catalyzed carbonaceous char and clay polystyrene nanocomposites with reinforced char were effectively created by Morgan et al. in 2002. The char by clay enforcement, according to them, has reduced the flammability of the polystyrene nanocomposites. Among the 0%, 2%, 5%, and 10% mass fractions employed in this investigation, the mass fraction of clay loading at 5% was in this instance the best percentage to be loaded for enhancing the heat release rates (Morgan, 2002). Multiwalled carbon nanotubes were found to improve the thermal stability of polyamide 12 according to Yuan et al. It was discovered that neat polyamide 12 underwent two stages of disintegration at 443°C and 462°C. The 1% loading of carbon nanotubes stabilized the polymer matrix compared to the starting stage of degradation because the carbon nanotube network successfully transferred heat energy between of polymer chains and carbon nanotube, preventing chemical disintegration of the polyamide 12 (Yuan, 2016).

3.4 Mechanical properties

Mohammad Farsi and colleagues investigated the characteristics of a biodegradable composite made of LCNFs and Pebax thermoplastic elastomer (LCNFs). LCNFs at various levels of 0%, 1%, 3%, and 5 were taken into account for this. The LCNFs were prepared in benzyl alcohol and then mixed with Pebax. In comparison to samples without LCNFs, the tensile strength, modulus, and impact strength of the polymer were raised by adding LCNFs. In comparison to samples lacking LCNFs, the tensile modulus of the samples dramatically increases as the concentration of LCNF increases from 1% to 5%. Once the content of LCNF was raised to 5%, the greatest modulus level (27.4 MPa) had been attained. Also, the average reduced from 24.3 to 23.34 MPa when the concentration of LCNF went from 1% to 3%, although the variance analysis found that this decrease was not statistically significant. The tensile strength was significantly affected by additional LCNF addition upto 5%, with 5% loading of LCNFs, yielding the maximum tensile strength. The outcomes demonstrated how LCNFs improved the polymer–LCNF matrix interactions (Farsi et al., 2018).

Anjum Saleem et al. created composites using melt-blended PEEK and PES thermoplastic polymers with CFs. They looked at the mechanical, thermal, and electrical characteristics of these composites. The addition of CFs improved the mechanical characteristics that are described in terms of storage modulus, loss, and damping. The storage modulus significantly increased as the filler content increased. The fillers' ability to facilitate stress transmission was the cause of this. The lower and higher temperatures of the loss modulus peaks indicated a better filler-matrix adhesion (Saleem et al., 2007). Microfibrillated cellulose was used as reinforcement in a composite made of PVA by Lu et al. After hours of stirring at 95°C, while adding increasing amounts of microfibrillated cellulose (1, 5, 10, and 15 wt.%), the mixture was allowed to cool to room temperature. Tensile strength and Young's modulus were shown to rise as MFC content increased up to 10 wt.%, but it decreases as the MFC level increases. At a 10 wt.% MFC concentration, the composite film's Young's modulus increased by 40% (Lu et al., 2008). Natalia Herrera et al. focused on the increase in compatibility and promoting nanofibrillation of fibers during melt compounding of thermoplastic biocomposites, and for this, chemical wood cellulose fiber modification is carried out. Two techniques were used for the grafting: the conventional bulk method and a novel technique that used acetic acid (AcOH) as the reaction solvent to enlarge the fiber structure during grafting. The use of AcOH as a solubilizing agent led to grafts that were highly dense both inside the nanostructure and across the volume of the HC wood cellulose fibers. As a result, it was found that the defibrillation of fibers into CNF during compounding was more apparent and that the CNF was distributed more evenly throughout the thermoplastic PCL matrix. Results show that with the addition of just 5 wt.% of fibers, the PCL's Young's modulus, strength, and toughness were all increased by over 60% (Herrera et al., 2020). Mechanical properties of lactic acid-based polymers can be very diverse, ranging from flexible and softer plastics to hard and extremely durable materials. Semicrystalline PLA is preferred over amorphous polymers when higher mechanical properties are desired. Semicrystalline

PLA has an approximate tensile modulus of 3 GPa, a flexural modulus of 5 GPa, a flexural strength of 100 MPa, and an approximated breaking elongation of 4% (Södergård & Stolt, 2002).

Sonker et al. created a PVA-based crosslinked composite with tungsten disulfide nanotube nanoparticle reinforcement and structural development by glutaric acid (GA) single-walled nano tubes (SWNTs). In order to add reinforcement, a SWNT was added to each of the three kinds of PVA films that were created: plain PVA, thermally cross-linked PVA (TH-CL-PVA), and GA crosslinked PVA (GA-CL-PVA). Both SWNT-TH-CL-PVA and SWNT-GA-CL-PVA exhibit maximum toughness of 85.68 MPa and maximum tensile strength of 139.9 MPa with a Young's modulus of 7.1 GPa, respectively (Sonker et al., 2016). A cellulose/PVA biocomposite film that has been processed with 1-n-butyl-3-methylimidazolium chloride was created by Abdulkhani et al. It was discovered that cellulose/PVA film's tensile strength is lower than that of cellulosic film (Abdulkhani et al., 2013). Nanocomposite based on PVA was created by Roohani et al. and reinforced with cotton linter-derived cellulose whiskers (0, 3, 6, 9, and 12 wt.% for PVA). According to studies on the tensile strength of nanocomposites under different relative humidity settings, the tensile modulus of nanocomposite films rose when the whisker content was raised for each relative humidity level. The tensile modulus significantly decreased with increase in humidity for a given filler quantity (Roohani et al., 2008). Nikmatin et al. investigated the influence of the nanoparticle-sized rattan filler on the mechanical, thermal, and physical parameters of the composite. All three types of PP—pure PP, PP with 5% rattan nanoparticles, and PP with 5% glass fiber (PP/FG5)—were considered. PP/FG5 and PP/R5 had greater elasticity and rupture moduli than the other material, although their tensile properties were comparable. A morphological analysis of the materials under consideration showed that PP/R5 had equally distributed components, the highest average hardness, the highest maximum strain, and the most advantageous ductile behavior (Nikmatin, 2017).

3.5 Conclusion

This chapter gives a general review of the thermoplastic polymer composites' physical, thermal, and mechanical properties. These days, thermoplastics are available in a wide range of shapes, each with a special set of fascinating characteristics. They can be produced to be transparent like glass, hard like metal and concrete, or flexible like rubber for use in a range of products. They function admirably as thermal and electrical insulators, have good corrosion resistance, and 'do not rust. Several studies conducted by a number of researchers are used to discuss physical, thermal, and mechanical qualities. Because they are lightweight, have high mechanical strength, and are resistant to environmental influences, thermoplastics are a wonderful material for many applications. These composite materials have an impact on a variety of applications, including packaging, automotive, light structures, civil engineering, aviation, sports, biomedicine, thermomechanical components, and aerospace.

Conflict of interest

There are no conflicts of interest to declare by the authors.

References

- Abdulkhani, A., Hojati Marvast, E., Ashori, A., Hamzeh, Y., & Karimi, A. N. (2013). Preparation of cellulose/polyvinyl alcohol biocomposite films using 1-n-butyl-3-methylimidazolium chloride. *International Journal of Biological Macromolecules*, *62*, 379–386, Elsevier BV.
- Ahmadijokani, F., Shojaei, A., Dordanihaghighi, S., Jafarpour, E., Mohammadi, S., & Arjmand, M. (2020). Effects of hybrid carbon-aramid fiber on performance of nonasbestos organic brake friction composites. *Wear*.
- Amrollahi, S., Ramezanzadeh, B., Yari, H., Ramezanzadeh, M., & Mahdavian, M. (2019). Synthesis of polyaniline-modified graphene oxide for obtaining a high performance epoxy nanocomposite film with excellent UV blocking/antioxidant/anti-corrosion capabilities. *Composites Part B: Engineering*, *173*, 106804.
- Arabbpour, A., Shockravi, A., Rezania, H., & Farahati, R. (2020). Investigation of anticorrosive properties of novel silane-functionalized polyamide/GO nanocomposite as steel coatings. *Surfaces and Interfaces*, *18*, 100453.
- Asim, M., Jawaid, M., Nasir, M., & Saba, N. (2018). Effect of fiber loadings and treatment on dynamic mechanical, thermal and flammability properties of pineapple leaf fiber and kenaf phenolic composites. *Journal of Renewable Materials*, *6*, 383–393.
- Baek, Y.-M., Shin, P.-S., Kim, J.-H., Park, H.-S., DeVries, K. L., & Park, J.-M. (2020). Thermal transfer, interfacial, and mechanical properties of carbon fiber/polycarbonate-CNT composites using infrared thermography. *Polymer Testing*, *81*, 106247.
- Chen, J., & Gao, X. (2019). Thermal and electrical anisotropy of polymer matrix composite materials reinforced with graphene nanoplatelets and aluminum-based particles. *Diamond and Related Materials*, *100*, 107571.
- Cheng, Q., Jiang, H., & Li, Y. (2020). Effect of fiber content and orientation on the scratch behavior of short glass fiber reinforced PBT composites. *Tribology International*, *146*, 106221.
- Dagdag, O., Hsissou, R., El Harfi, A., Safi, Z., Berisha, A., Verma, C., et al. (2020). Epoxy resins and their zinc composites as novel anti-corrosive materials for copper in 3% sodium chloride solution: Experimental and computational studies. *Journal of Molecular Liquids*, *315*, 113757.
- Dagdag, O., Safi, Z., Hsissou, R., Erramli, H., El Bouchti, M., Wazzan, N., et al. (2019). Epoxy prepolymers as new and effective materials for corrosion inhibition of carbon steel in acidic medium: Computational and experimental studies. *Scientific Reports*, *9*, 1–14.
- Das, P., & Tiwari, P. (2019). Thermal degradation study of waste polyethylene terephthalate (PET) under inert and oxidative environments. *Thermochimica Acta*, *679*, 178340.
- Datsyuk, V., Trotsenko, S., Trakakis, G., Boden, A., Vyzas-Asimakopoulos, K., Parthenios, J., et al. (2020). Thermal properties enhancement of epoxy resins by incorporating polybenzimidazole nanofibers filled with graphene and carbon nanotubes as reinforcing material. *Polymer Testing*, *82*, 106317.
- De, S., Fulmali, A. O., Shivangi, P. N., Choudhury, S., Prusty, R. K., & Ray, B. C. (2020). Interface modification of carbon fiber reinforced epoxy composite by hydroxyl/carboxyl functionalized carbon nanotube. *Materials Today: Proceedings*, *2020/04/03/*.

- Devnani, G. L., & Sinha, S. (2019). Effect of nanofillers on the properties of natural fiber reinforced polymer composites. *Materials Today: Proceedings*, 18, 647–654.
- Dong, Z.-J., Zhou, T., Luan, H., Williams, R. C., Wang, P., & Leng, Z. (2019). Composite modification mechanism of blended bio-asphalt combining styrene-butadiene-styrene with crumb rubber: A sustainable and environmental-friendly solution for wastes. *Journal of Cleaner Production*, 214, 593–605.
- El Gouri, M., El Bachiri, A., Hegazi, S. E., Rafik, M., & El Harfi, A. (2009). Thermal degradation of a reactive flame retardant based on cyclotriphosphazene and its blend with DGEBA epoxy resin. *Polymer Degradation and Stability*, 94, 2101–2106.
- Farsi, M., Tavasoli, A., Yousefi, H., & Tabari, H. Z. (2018). A study on the thermal and mechanical properties of composites made of nanolignocellulose and Pebax® polymer. *Journal of Thermoplastic Composite Materials*, 32(11), 1509–1524.
- Goffin, A.-L., et al. (2011). Poly (ϵ -caprolactone) based nanocomposites reinforced by surface-grafted cellulose nanowhiskers via extrusion processing: Morphology, rheology, and thermo-mechanical properties. *Polymer*, 52(7), 1532–1538.
- Helen, M., Viswanathan, B., & Srinivasa Murthy, S. (2006). Fabrication and properties of hybrid membranes based on salts of heteropolyacid, zirconium phosphate and polyvinyl alcohol. *Journal of Power Sources*, 163(1), 433–439.
- D.E. Henton, P. Gruber, J. Lunt, J. Randall (2005). in: A.K. Mohanty, M. Misra, L.T. Drzal (Eds), Natural fibers, biopolymers, and biocomposites, Taylor & Francis, Boca Raton, pp. 527–577.
- Herrera, N., Olsén, P., & Berglund, L. A. (2020). Strongly improved mechanical properties of thermoplastic biocomposites by PCL Grafting inside holocellulose wood fibers. *ACS Sustainable Chemistry & Engineering*, 8(32), 11977–11985.
- Hsissou, R., About, S., Safi, Z., Benhiba, F., Wazzan, N., Guo, L., et al. (2021). Synthesis and anticorrosive properties of epoxy polymer for CS in [1 M] HCl solution: Electrochemical, AFM, DFT and MD simulations. *Construction and Building Materials*, 270, 121454.
- Hsissou, R., About, S., Seghiri, R., Rehioui, M., Berisha, A., Erramli, H., et al. (2020). Evaluation of corrosion inhibition performance of phosphorus polymer for carbon steel in [1M] HCl: Computational studies (DFT, MC and MD simulations). *Journal of Materials Research and Technology*, 9, 2691–2703.
- Hsissou, R., Bekhta, A., & El Harfi, A. (2017). Viscosimetric and rheological studies of a new trifunctional epoxy pre-polymer with noyan ethylene: Triglycidyl Ether of Ethylene of Bisphenol A (TGEEBA). *Journal of Materials and Environmental Sciences*, 8, 603–610.
- Hsissou, R., Bekhta, A., & El Harfi, A. (2018). Synthesis and characterization of a new epoxy resin homologous of DGEBA: Diglycidyl bis disulfide carbon ether of bisphenol A. *Journal of Chemical Technology and Metallurgy*, 53, 414–421.
- Hsissou, R., Bekhta, A., Elharfi, A., Benzidia, B., & Hajjaji, N. (2018). Theoretical and electrochemical studies of the coating behavior of a new epoxy polymer: Hexaglycidyl ethylene of methylene dianiline (HGEMDA) on E24 steel in 3.5% NaCl. *Portugaliae Electrochimica Acta*, 36, 101–117.
- Hsissou, R., Benassaoui, H., Benhiba, F., Hajjaji, N., & El Harfi, A. (2017). Application of a new trifunctional epoxy prepolymer, triglycidyl ethylene ether of bisphenol A, in the coating of E24 steel in 3.5% NaCl. *Journal of Chemical Technology and Metallurgy*, 52, 431–438.
- Hsissou, R., Dagdag, O., About, S., Benhiba, F., Berradi, M., El Bouchti, M., et al. (2019). Novel derivative epoxy resin TGETET as a corrosion inhibition of E24 carbon steel in 1.0 M HCl solution. Experimental and computational (DFT and MD simulations) methods. *Journal of Molecular Liquids*, 284, 182–192.

- Hsissou, R., El Bouchti, M., & Elharfi, A. (2017). Elaboration and viscosimetric, viscoelastic and rheological studies of a new hexafunctional polyepoxide polymer: Hexaglycidyl ethylene of methylene dianiline. *Journal of Materials and Environmental Sciences*, 8, 4349–4361.
- Hsissou, R., & El Harfi, A. (2018). Elaboration and rheological study of a new trifunctional polyepoxide macromolecular binder. *Journal of Chemical Technology and Metallurgy*, 53, 170–176.
- Hsissou, R., Seghiri, R., Benzekri, Z., Hilali, M., Rafik, M., & Elharfi, A. (2021). *Polymer composite materials: A comprehensive review*, . *Composite structures* (262), p. 113640. Elsevier BV.
- Kaushik, A., Singh, M., & Verma, G. (2010). Green nanocomposites based on thermoplastic starch and steam exploded cellulose nanofibrils from wheat straw. *Carbohydrate Polymers*, 82(2), 337–345.
- Khalil, H. A., Jawaid, M., & Bakar, A. A. (2011). Woven hybrid composites: Water absorption and thickness swelling behaviours. *BioResources*, 6, 1043–1052.
- Khalil, H. A., Tehrani, M., Davoudpour, Y., Bhat, A., Jawaid, M., & Hassan, A. (2013). Natural fiber reinforced poly (vinyl chloride) composites: A review. *Journal of Reinforced Plastics and Composites*, 32, 330–356.
- Le Guen, M. J., Newman, R. H., Fernyhough, A., Emms, G. W., & Staiger, M. P. (2016). The damping–modulus relationship in flax–carbon fibre hybrid composites. *Composites Part B: Engineering*, 89, 27–33.
- Li, Y., Yi, X., Yu, T., & Xian, G. (2018). An overview of structural-functional-integrated composites based on the hierarchical microstructures of plant fibers. *Advanced Composites and Hybrid Materials*, 1, 231–246.
- Lu, J., Wang, T., & Drzal, L. T. (2008). Preparation and properties of microfibrillated cellulose polyvinyl alcohol composite materials. *Composites Part A: Applied Science and Manufacturing*, 39(5), 738–746, Elsevier BV.
- McKeen, L. W. (2014). *Plastics used in medical devices. Handbook of polymer applications in medicine and medical devices* (pp. 21–53). Elsevier.
- Middleton, J. C., & Tipton, A. J. (2000). Synthetic biodegradable polymers as orthopedic devices. *Biomaterials*, 21(23), 2335–2346, Elsevier BV.
- Morgan, A. B., et al. (2002). Flammability of polystyrene layered silicate (clay) nanocomposites: Carbonaceous char formation. *Fire and Materials*, 26(6), 247–253.
- Nikmatin, S., et al. (2017). Physical, thermal, and mechanical properties of polypropylene composites filled with rattan nanoparticles. *Journal of Applied Research and Technology*.
- Park, S.-J., & Heo, G.-Y. (2014). *Precursors and manufacturing of carbon fibers*, . *Superconductivity; springer series in materials science and business media* (Vol. 210, pp. 31–66). Dordrecht, The Netherlands: Springer.
- Rajak, D. K., Pagar, D. D., Menezes, P. L., & Linul, E. (2019). Fiber-reinforced polymer composites: Manufacturing, properties, and applications. *Polymers*, 11, 1667.
- Rod, K. A., Nguyen, M.-T., Elbakhshwan, M., Gills, S., Kutchko, B., Varga, T., et al. (2019). Insights into the physical and chemical properties of a cement-polymer composite developed for geothermal wellbore applications. *Cement and Concrete Composites*, 97, 279–287.
- Roohani, M., Habibi, Y., Belgacem, N. M., Ebrahim, G., Karimi, A. N., & Dufresne, A. (2008). Cellulose whiskers reinforced polyvinyl alcohol copolymers nanocomposites. *European Polymer Journal*, 44(8), 2489–2498. Available from <https://doi.org/10.1016/j.eurpolymj.2008.05.024>.

- Saleem, A., Frommann, L., & Iqbal, A. (2007). High performance thermoplastic composites: Study on the mechanical, thermal, and electrical resistivity properties of carbon fiber-reinforced polyetheretherketone and polyethersulphone. *Polymer Composites*, 28(6), 785–796.
- Sonker, A. K., Wagner, H. D., Bajpai, R., Tenne, R., & Sui, X. M. (2016). Effects of tungsten disulphide nanotubes and glutaric acid on the thermal and mechanical properties of polyvinyl alcohol. *Composites Science and Technology*, 127, 47–53.
- Södergård, A., & Stolt, M. (2002). Properties of lactic acid based polymers and their correlation with composition. *Progress in Polymer Science*, 27(6), 1123–1163.
- Tarhini, A. A., & Tehrani-Bagha, A. R. (2019). Graphene-based polymer composite films with enhanced mechanical properties and ultra-high in-plane thermal conductivity. *Composites Science and Technology*, 184, 107797.
- Kumar, R. M., & Rajini, N. (2019). Thermal properties of thermoplastic rubber (TPR) reinforced with polytetrafluoroethylene (PTFE) particle polymer composite. *International Journal of Recent Technology and Engineering*, 8(4S2), 983–986.
- Tian, H., Yan, J., Rajulu, A. V., Xiang, A., & Luo, X. (2017). Fabrication and properties of polyvinyl alcohol/starch blend films: Effect of composition and humidity. *International Journal of Biological Macromolecules*, 96, 518–523.
- Vaggar, G. B., & Kamate, S. C. (2019). Thermal property characterization for enhancement of thermal conductivity of hybrid polymer composites. *Materials Today: Proceedings*.
- Van de Velde, K., & Kiekens, P. (2002). Biopolymers: Overview of several properties and consequences on their applications. *Polymer Testing*, 21(Issue 4), 433–442.
- Venkateshwaran, N., & Elayaperumal, A. (2010). Banana fiber reinforced polymer composites-a review. *Journal of Reinforced Plastics and Composites*, 29, 2387–2396.
- Wu, H., & Drzal, L. T. (2016). Multifunctional highly aligned graphite nanoplatelet-polyether imide composite in film form. *Materials Chemistry and Physics*, 182, 110–118.
- Yao, S.-S., Jin, F.-L., Rhee, K. Y., Hui, D., & Park, S.-J. (2018). Recent advances in carbon-fiber-reinforced thermoplastic composites: A review. *Composites Part B: Engineering*, 142, 241–250.
- Yuan, S., et al. (2016). Highly enhanced thermal conductivity of thermoplastic nanocomposites with a low mass fraction of MWCNTs by a facilitated latex approach. *Composites Part A: Applied Science and Manufacturing*, 90, 699–710.
- Zhang, T., Sun, J., Ren, L., Yao, Y., Wang, M., Zeng, X., et al. (2019). Nacre-inspired polymer composites with high thermal conductivity and enhanced mechanical strength. *Composites Part A: Applied Science and Manufacturing*, 121, 92–99.
- Zheng, S., Bellido-Aguilar, D. A., Hu, J., Huang, Y., Zhao, X., Wang, Z., et al. (2019). Waterborne bio-based epoxy coatings for the corrosion protection of metallic substrates. *Progress in Organic Coatings*, 136, 105265.